

Highlights

Computational and numerical analysis of AC optimal power flow formulations on large-scale power grids

Arun Sukumaran Nair,Shrirang Abhyankar,Slaven Peles,Prakash Ranganathan

- An in-depth comparison of the AC-OPF model for three formulations: power balance polar, power balance Cartesian and current balance Cartesian presenting their characteristic differences.
- Comparison of structural differences in terms of number of variables, constraints and non-zeros in Jacobian and hessian matrix.
- Numerical and computational performance evaluation for the AC-OPF formulations on nine different test cases including large-scale synthetic U.S. networks.

Computational and numerical analysis of AC optimal power flow formulations on large-scale power grids^{*}

Arun Sukumaran Nair^a, Shirang Abhyankar^b, Slaven Peles^b and Prakash Ranganathan^a

^aDepartment of Electrical Engineering, University of North Dakota, Grand Forks, ND, USA

^bPacific Northwest National Laboratory, Richland, WA, USA

ARTICLE INFO

Keywords:

AC Optimal Power Flow
Large-Scale power grids
Formulation
Grid Operation
Optimization

ABSTRACT

Alternating current optimal power flow (AC-OPF) is a fundamental tool in electric utilities to determine optimal operation of the various resources. Typically, the AC-OPF problem uses power balance formulation containing voltages and power equations. Yet, there is no comprehensive comparison of the different AC-OPF formulations, especially for large-scale networks. This paper presents a detailed comparative evaluation of different formulations of the AC-OPF problem on networks ranging from 9-bus to 25,000 buses. Three different formulations: 1) power balance with polar voltages, 2) power balance with Cartesian voltages, and 3) current balance with Cartesian voltages are discussed in detail by comparing their characteristics, and numerical and computational performance.

1. Introduction

Optimal Power Flow (OPF) is a fundamental tool used in power industry to ensure an optimal and secure operation of the grid. Its usage is pervasive in the industry with applications spanning across transmission and distribution, real-time and day-ahead operations, and short-term and long-term planning. With the expansion and proliferation of renewable energy resources, introduction of additional monitoring and control introduced by smart grid initiatives, and increased interaction between transmission and distribution, the grid operators are facing additional challenges to operate the grid securely at least cost. The OPF is a fundamental tool at the disposal of grid operators and engineers to ensure this secure and optimal operation [29]. However, with the increased complexities, the OPF tools will need to be more robust and faster.

While the performance of power grid applications, such as the OPF need to be improved, one must also take into account the rapid growth and change in the computing industry. The computing industry has grown leaps and bounds after the OPF was first developed in the 1960's by Carpentier *et al.* [9, 42]. It has gone through the era of mainframe computers, distributed memory clusters with single core nodes, clusters with multicore nodes, and now distributed memory clusters with heterogeneous nodes with multiple processors and accelerators. The next revolution in the computing industry, which has already commenced, is on the heavy usage of hardware accelerators, such as Graphical Processing Units (GPUs) spurred by the gaming industry and machine-learning applications. This new technology has dramatically improved computational performance, but at the same time it has imposed new constraints on how mathematical models can be effectively implemented. Under such a changing

computing environment, it is prudent to revisit the power grid applications and assess the building blocks of these applications and ways to adapt them to these newer architectures.


This paper attempts at assessing these fundamental building blocks for the AC optimal power flow (AC-OPF) application. We provide an in-depth comparison of three different formulations for AC-OPF – power-balance with polar voltages, power-balance with Cartesian voltages, and current-balance with Cartesian voltages – and compare their structure and characteristics. In addition, we present the numerical and computational performance of these formulations to highlight their differences, point to the most efficient formulation, and provide benchmark comparison metrics on very-large networks. The significant distinguishing contributions can be summarized as follows

- An in-depth comparison of the AC-OPF model for three formulations: power balance polar, power balance Cartesian and current balance Cartesian presenting their characteristic differences.
- Comparison of structural differences in terms of number of variables, constraints and non-zeros in Jacobian and hessian matrix.
- Numerical and computational performance evaluation for the AC-OPF formulations on nine different test cases including large-scale synthetic U.S. networks [7].

The OPF application code developed in this work is written in C language using the numerical computing library PETSc [4, 5]. For validation, the results from the three model formulations are compared with MATPOWER [49]. Note that the MATPOWER utilizes the power balance polar formulation for the AC-OPF model.

The remainder of the paper is structured as follows: In section 2, a literature survey on the different formulations of AC optimal power flow, and the solution techniques is presented. Section 3 presents the compact AC-OPF form as a

^{*}The authors acknowledge the support of the Pacific Northwest National Lab (PNNL) and National Science Foundation (NSF), award #1537565 for this work.

 arun.sukumaranair@und.edu (A.S. Nair)

ORCID(s):

Nomenclature

n_g	Number of generators in the network
n_b	Number of buses in the network
n_{br}	Number of branches in the network
n_l	Number of loads in the network
$\alpha_k, \beta_k, \gamma_k$	Generator k cost-coefficients
G_k	K^{th} Generator G
V_i	Voltage magnitude at bus i
θ_i	Voltage angle at bus i
θ_{ref}	Reference bus angle
θ_{ref0}	Reference bus angle constant
\bar{V}_i	Complex voltage at a bus
V_{Ri}	Real part of the complex voltage,
V_{Ii}	Imaginary parts of the complex voltage
V_i^+	Upper bound on voltage magnitude
V_i^-	Lower bound on voltage magnitude
G_{ff}	Self conductance for line ft
G_{ft}	Mutual conductance for the line ft
B_{ff}	Self susceptance of the line ft
B_{ft}	Mutual susceptance of the line ft
P_{Gk}	Real power output for generator k
Q_{Gk}	Reactive power output for generator k
P_{Gk}^+	Upper bound on generator real power output
P_{Gk}^-	Lower bound on generator real power output
Q_{Gk}^+	Upper bound on generator reactive power output
Q_{Gk}^-	Lower bound on generator reactive power output
P_{ft}	Real power flow from bus f to bus t on line ft
Q_{ft}	Reactive power flow from bus f to bus t on line ft
P_{tf}	Real power flow from bus t to bus f on line ft
Q_{tf}	Reactive power flow from bus t to bus f on line ft
S_f	Apparent power flow from bus f to bus t on line ft
S_t	Apparent power flow from bus t to bus f on line ft
S_{ft}^+	Upper bound on apparent power
A_{br}	Branch incidence matrix
A_G	Generator incidence matrix
A_L	Load incidence matrix

general NLP problem and then dives into the detailed modeling of the three different formulations. Section 4 describes the test cases utilized for the study and section 5 summarizes the modeling and performance results from the evaluations. We conclude with a brief discussion of the results in section 6. The appendix provides a detailed information about the AC-OPF code run and the number of non-zeros in Jacobian and Hessian parameters are given in tables 4 and 5 respectively.

2. AC-OPF literature review

The Optimal Power Flow (OPF) ensures a secure operation of electric power plants for a given transmission network with, typically, the objective of minimizing generation cost subjected to operational and security constraints in the network [21]. It is one of the most important tools used by engineers for power system operation and planning. AC-OPF is an optimization model that considers the full AC power flow equations. It is the most accurate representation of power flow in a network assuming the model parameters

are correct. Compared to a DC optimal power flow, the benefits of AC-OPF are increased accuracy, inclusion of reactive power, current, voltage and losses in the network (e.g. transmission losses, active and reactive power load loss)[12, 17]. AC-OPF plays a critical role in the operation of Independent System Operator (ISO) power markets [8]. It is utilized in every important stage of a power system operation and planning such as expansion planning [45], grid management [40], day ahead markets [28], and also for real-time control [25]. AC-OPF is performed yearly for capacity expansion, daily for day-ahead markets, and, in some cases, even for every 5 minutes. An extensive review on the application of AC-OPF in distributed generation planning and operation is provided in [33].

However, AC-OPF remains a computationally complex problem, still lacking a fast and robust solution even after 50 years of its formulation. The problem is getting more complicated with the introduction of distributed and large scale renewable energy sources [20, 31, 32, 48]. The current approach utilizes decomposition, approximations and assumptions for a fast and acceptable solution [10]. Researchers have explored different methods such as linear approximation [11, 37, 1, 38], conic formulation [6, 19], semidefinite programming [44, 26], quadratic convex relaxation [14], decomposition [27, 39] for a faster solution. A detailed study on the effect of inexact convex relaxation in AC-OPF feasibility is given [43]. The approaches of approximations and assumptions cost the companies in millions of dollars in operational cost, damage to the environment from unnecessary emissions and energy waste. Even a small improvement in dispatch efficiency can result in cost savings in the order of billions of dollars [11]. Studies have shown that a 5% improvement in AC-OPF solution can yield an estimated savings of over twenty billion dollar in the US market [8].

Most of the AC-OPF literature utilize the polar power - voltage formulation first introduced by Carpentier in the 1960's. The other two main formulations of OPF are rectangular power-voltage and rectangular current-voltage formulations. Researchers have also explored other formulations of OPF such as current injection and a mix of polar and rectangular coordinates [24, 22]. The hybrid method in [24] used rectangular forms of voltage and current, current mismatch equations for power balance and numerical stability is ensured by PV buses. The equivalent current injection based method also utilized a decoupled optimization for faster processing. M. Jereminov *et al.* [22] proposed a solution methodology for AC-OPF using equivalent circuit formulation. The AC-OPF is represented as a non-linear equivalent circuit in which generator model is represented by conductance and susceptance state variables and network constraints handled by the generator admittance state variables. The proposed method solves the convergence problem in the current balance Cartesian formulation.

In [1], authors present a linear approximation method to solve AC-OPF in power balance polar formulation using the Mixed Integer Linear Programming (MILP) approach. The method of binary expansion discretisation is used to convert

the non-linear AC-OPF in to linear problem without losing accuracy. The method had the advantage of obtaining reactive power and voltage profile at the same time but faced exponential increase in execution time with CPLEX solver. An approximation of AC-OPF in power balance polar formulation utilizing Langrangian dual is proposed in [20]. A Supervised Deep Learning model with rectified linear unit (ReLU) activation function is modeled to generate the generator set-points. The proposed approximation method had a better accuracy and a faster processing time than DC-OPF.

Y. Tang *et al.* in [41] proposed a real-time AC-OPF based on quasi-Newton methods using the current balance Cartesian formulation. The approach utilised the second-order information to provide sub-optimal solutions for real-time applications. A small correction term is used to track the optimal solution assuming a single-phase power flow. The superiority of linear approximation of AC-OPF in current balance Cartesian over traditional quadratic power flow formulation is stated in [34]. It proposes the idea of using AC-OPF in current balance form and its approximations for practical applications for its improved computational performance. A continuation method (homotopy) is used in [15] to covert the DC OPF solution in to AC-OPF by slowly increasing the non-linearities in equality and inequality constraints. The proposed method achieved robust solution with a reasonable computational overhead.

A comparative analysis of different power flow methodologies is performed in [16], but on Power Flow (PF) problem. The authors tested the performance of the formulations on well-conditioned and ill-conditioned networks. A 118, 300 and 730 were used to test these methods and for well-conditioned networks all the three methodologies showed almost similar performance. The slight performance improvement in power balance polar and current balance Cartesian methods are noted in the work. In the case of ill-conditioned networks rectangular based formulations had better convergence properties. A comparison of three different solvers over different power flow formulations are implemented in [36]. The performance of KNITRO, MATPOWER's MIPS (MATPOWER Interior Point Solver) and FMINCON (Find minimum of constrained nonlinear multivariable function) methods over different bus systems and formulations are presented in this paper. In [35], authors performed a comparative analysis of three different AC-OPF formulation with different generator capability curves, solvers and initial conditions. The evaluations are done on 118 and 2736 bus systems. In the studies, power balance polar and current balance Cartesian performed better in terms of computational time. In case of solvers IPOPTH and KNITRO performed the best and for initial conditions midpoint and flat start as the best choice for AC-OPF.

3. Problem formulations

General form for an ACOPF formulation is shown in eqs. (1) to (4). It is an optimization model with a minimization objective subjected to a set of equality and inequality constraints. The objective function in AC-OPF can be

modelled for the minimization cost, minimization of losses, maintaining constant voltage profile, transmission planning or a combination of objectives.

$$\min_x f(x) \quad (1)$$

subject to

$$g(x) = 0 \quad (2)$$

$$h(x) \leq 0 \quad (3)$$

$$x^{min} \leq x \leq x^{max} \quad (4)$$

Here, $f(x)$ denotes the objective function for minimizing the generation cost and active and reactive power load losses. $g(x)$ represents the nodal power flow balance equations, the inequality constraint $h(x)$ models the branch flow limits and the bounds in eq. (4) limits the voltage magnitudes, generator power injections and reference bus angles [23, 12].

3.1. Power Balance Polar Formulation

Here, AC-OPF does a minimization of the generation cost and the objective function used in the formulation is shown in eq. (5). The generation cost is assumed to be a polynomial function of order 2.

$$C = \sum_{k=1}^{n_g} \alpha_k P_{G_k}^2 + \beta_k P_{G_k} + \gamma_k \quad (5)$$

This formulation employs the polar representation of voltage with voltage magnitude at bus i is V_i and angle θ_i . The equality constraints are shown in eqs. (6) and (7) and the inequality constraints in eqs. (8) to (10) [16, 1].

$$\begin{aligned} \sum_{A_{br}(f,t)=1} (G_{ff}(V_f^2) + V_f V_t (G_{ft} \cos(\theta_f - \theta_t) \\ + B_{ft} \sin(\theta_f - \theta_t)) - \sum_{A_G(f,k)=1} P_{Gk} \\ + \sum_{A_L(f,j) \neq 0} P_{Dj} = \Delta P_f = 0 \end{aligned} \quad (6)$$

$$\begin{aligned} \sum_{A_{br}(f,t)=1} (-B_{ff}(V_f^2) + V_f V_t (G_{ft} \sin(\theta_f - \theta_t) \\ - B_{ft} \cos(\theta_f - \theta_t)) - \sum_{A_G(f,k) \neq 0} Q_{Gk} \\ + \sum_{A_L(f,j)=1} Q_{Dj} = \Delta Q_f = 0 \end{aligned} \quad (7)$$

$$V_i^- \leq V_i \leq V_i^+ \quad (8)$$

$$P_{Gk}^- \leq P_{Gk} \leq P_{Gk}^+ \quad (9)$$

$$Q_{Gk}^- \leq Q_{Gk} \leq Q_{Gk}^+ \quad (10)$$

$$0 \leq S_f^2 \leq (S_{ft}^+)^2 \quad (11)$$

$$0 \leq S_t^2 \leq (S_{ft}^+)^2 \quad (12)$$

The eqs. (8) to (10), represents the bounds on the voltage magnitude, active power and reactive power injection at each bus. The bounds on the apparent power flows in the network are shown in eqs. (11) and (12). For the model, the reference angle is held constant ($\theta_{ref} = \theta_{ref0}$).

$$S_f = \sqrt{P_{ft}^2 + Q_{ft}^2} \quad (13)$$

$$S_t = \sqrt{P_{tf}^2 + Q_{tf}^2} \quad (14)$$

$$P_{ft} = G_{ff}(V_f^2) + V_f(G_{ft}V_t \cos(\theta_f - \theta_t) + V_t B_{ft} \sin(\theta_f - \theta_t)) \quad (15)$$

$$Q_{ft} = -B_{ff}(V_f^2) + V_f(G_{ft}V_t \sin(\theta_f - \theta_t) - V_t B_{ft} \cos(\theta_f - \theta_t)) \quad (16)$$

$$P_{tf} = G_{tt}(V_t^2) + V_t(G_{tf}V_f \cos(\theta_t - \theta_f) + V_f B_{tf} \sin(\theta_t - \theta_f)) \quad (17)$$

$$Q_{tf} = -B_{tt}(V_t^2) + V_t(G_{tf}V_f \sin(\theta_t - \theta_f) - V_f B_{tf} \cos(\theta_t - \theta_f)) \quad (18)$$

The eqs. (13) to (18) model the apparent power flows in the network.

3.2. Power Balance Cartesian

In this formulation, the voltage at each bus takes the Cartesian form, the real and imaginary part of the voltage are represented by V_{Ri}, V_{Ii} respectively ($\tilde{V}_i = V_{Ri} + \sqrt{-1}V_{Ii}$). The objective function to be minimized remains the same as in eq. (5). The constraints are listed in eqs. (19) to (25).

$$\begin{aligned} \sum_{A_{br}(f,t)=1} (G_{ff}(V_{Rf}^2 + V_{If}^2) + V_{Rf}(G_{ft}V_{Rt} - B_{ft}V_{It}) \\ + V_{If}(B_{ft}V_{Rt} + G_{ft}V_{It})) - \sum_{A_G(f,k)=1} P_{Gk} \\ + \sum_{A_L(f,j) \neq 0} P_{Dj} = \Delta P_f = 0 \end{aligned} \quad (19)$$

$$\begin{aligned} \sum_{A_{br}(f,t)=1} (-B_{ff}(V_{Rf}^2 + V_{If}^2) + V_{If}(G_{ft}V_{Rt} - B_{ft}V_{It}) \\ - V_{Rf}(B_{ft}V_{Rt} + G_{ft}V_{It})) - \sum_{A_G(f,k) \neq 0} Q_{Gk} \\ + \sum_{A_L(f,j)=1} Q_{Dj} = \Delta Q_f = 0 \end{aligned} \quad (20)$$

$$(V_i^-)^2 \leq V_i^2 = V_{Ri}^2 + V_{Ii}^2 \leq (V_i^+)^2 \quad (21)$$

$$P_{Gk}^- \leq P_{Gk} \leq P_{Gk}^+ \quad (22)$$

$$Q_{Gk}^- \leq Q_{Gk} \leq Q_{Gk}^+ \quad (23)$$

$$0 \leq S_f^2 \leq (S_{ft}^+)^2 \quad (24)$$

$$0 \leq S_t^2 \leq (S_{ft}^+)^2 \quad (25)$$

where the maximum flow S^+ is either the normal, short-term, or emergency rating of the line. The apparent power flows S_f and S_t at the from and to ends of the line are given by eqs. (26) to (31).

$$S_f = \sqrt{P_{ft}^2 + Q_{ft}^2} \quad (26)$$

$$S_t = \sqrt{P_{tf}^2 + Q_{tf}^2} \quad (27)$$

$$P_f = G_{ff}(V_{Rf}^2 + V_{If}^2) + V_{Rf}(G_{ft}V_{Rt} - B_{ft}V_{It}) + V_{If}(B_{ft}V_{Rt} + G_{ft}V_{It}) \quad (28)$$

$$Q_f = -B_{ff}(V_{Rf}^2 + V_{If}^2) + V_{If}(G_{ft}V_{Rt} - B_{ft}V_{It}) - V_{Rf}(B_{ft}V_{Rt} + G_{ft}V_{It}) \quad (29)$$

$$P_t = G_{tt}(V_{Rt}^2 + V_{It}^2) + V_{Rt}(G_{tf}V_{Rf} - B_{tf}V_{If}) + V_{It}(B_{tf}V_{Rf} + G_{tf}V_{If}) \quad (30)$$

$$Q_t = -B_{tt}(V_{Rt}^2 + V_{It}^2) + V_{It}(G_{tf}V_{Rf} - B_{tf}V_{If}) - V_{Rt}(B_{tf}V_{Rf} + G_{tf}V_{If}) \quad (31)$$

Table 1
AC-OPF Formulation Comparison.

	Power balance Polar	Power balance Cartesian	Current balance Cartesian
Variables	$ v_i , \theta_i, P_G, Q_G, P, Q$	V_R, V_I, P_G, Q_G, P, Q	$V_{Ri}, V_{Ii}, P_G, Q_G, I_R, I_I$
No. of variables	$2n_b + 2n_{br} + 2n_g$	$2n_b + 2n_{br} + 2n_g$	$2n_b + 2n_{br} + 2n_g$
Network constraints	$2n_b$ Nonlinear	$2n_b$ Quadratic	$2n_b$ locally nonlinear
Network Jacobian	Nonlinear	Linear	locally nonlinear
Voltage magnitude constraints	Variable limit	Non-convex quadratic inequalities	Non-convex quadratic inequalities
No. of equations	$2n_b + 4n_{br}$ (Equality) $2n_b + 4n_{br} + 4n_g$ (Inequality)	$2n_b + 4n_{br}$ (Equality) $2n_b + 2n_{br} + 4n_g$ (Inequality)	$2n_b + 2n_{br}$ (Equality) $2n_b + n_{br} + 4n_g$ (Inequality)

3.3. Current Balance Cartesian

This formulation employs a set of equations in current injection equations written in rectangular coordinates [16, 2]. The objective function remains the same as in eq. (5) and the constraints are listed in equations eqs. (32) to (38). The equations for apparent power takes the form as shown previously in eqs. (26) to (31).

$$\begin{aligned} \sum_{A_{br}(f,t)=1} (G_{ft}V_{Rt} - B_{ft}V_{It}) - \left(\sum_{A_G(f,k)=1} P_{Gk} \right. \\ \left. - \sum_{A_L(f,j) \neq 0} P_{Dj} \right) V_{Rf} / (V_{Rf}^2 + V_{If}^2) \\ - \left(\sum_{A_G(f,k)=0} Q_{Gk} - \sum_{A_L(f,j) \neq 1} Q_{Dj} \right) \\ V_{If} / (V_{Rf}^2 + V_{If}^2) = 0 \end{aligned} \quad (32)$$

$$\begin{aligned} \sum_{A_{br}(f,t)=1} (G_{ft}V_{It} + B_{ft}V_{Rt}) - \left(\sum_{A_G(f,k)=1} P_{Gk} \right) \\ - \sum_{A_L(f,j) \neq 0} P_{Dj} \right) V_{If} / (V_{Rf}^2 + V_{If}^2) \\ + \left(\sum_{A_G(f,k)=0} Q_{Gk} - \sum_{A_L(f,j) \neq 1} Q_{Dj} \right) \\ V_{Rf} / (V_{Rf}^2 + V_{If}^2) = 0 \end{aligned} \quad (33)$$

$$(V_i^-)^2 \leq V_i^2 = V_{Ri}^2 + V_{Ii}^2 \leq (V_i^+)^2 \quad (34)$$

$$P_{Gk}^- \leq P_{Gk} \leq P_{Gk}^+ \quad (35)$$

$$Q_{Gk}^- \leq Q_{Gk} \leq Q_{Gk}^+ \quad (36)$$

$$0 \leq S_{ft}^2 \leq (S_{ft}^+)^2 \quad (37)$$

$$0 \leq S_t^2 \leq (S_{ft}^+)^2 \quad (38)$$

3.4. Model Comparison

The table 1 lists the model parameters from the three formulations of AC-OPF [8]. All the three formulation have the same number of variables in the optimization model. In case of power balance polar representation, it has a set of $2n_b$ non-linear equality constraints with sine, cosine functions and quadratic terms that apply throughout the grid. The formulation has a non-linear network Jacobian and variable limit on the voltage magnitude. The power balance Cartesian formulation models the system with $2n_b$ non-linear equality constraints with quadratic terms. The system has non-convex quadratic inequalities at bus and non-convex inequalities at each set of connected buses. The current balance Cartesian formulation employs locally linear equality and non-convex inequalities at each bus.

4. Test Cases

The three formulations of AC-OPF are tested on 9 different bus systems. The case 1 is a 9-bus, 3 generator model based on the data from [13]. The case 2, the 39-bus New England system with generator types of fossil, hydro, nuclear and network interconnections [3]. The IEEE 118 and IEEE 300 bus system models are the 4th and 5th test case. The 500 bus system network is a synthetic model to mimic the 138 and 300 kV transmission network in the northwestern part of South Carolina. The synthetic 2000 bus case is a representation of the 161, 230, 500 kV transmission network in the state of Texas [7]. The 3120 bus system is a representation of the Polish system during the morning peak in summer 2008. A synthetic representation of a part of the Western Electricity Coordinating Council (WECC) system transmission network with 115, 138, 161, 230, 345, 500, 765 kV lines is modelled in the 10,000 bus system case. The synthetic 25,000 bus system case is a representation of the North-East Mid-Atlantic region transmission network in US [7]. The table 2 lists the features of the 9 different test cases used in this study.

5. Numerical and Computational Performance

The optimization problem is solved using the Ipopt library [46]. Ipopt is a widely-used open source software library for solving large-scale non-linear optimization prob-

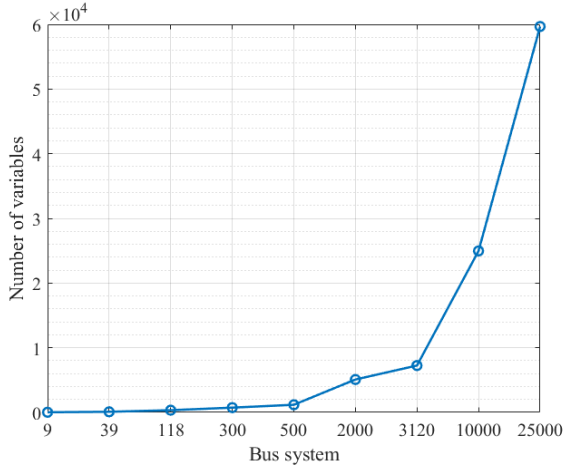
Table 2

The different bus systems utilized for the analysis.

Test Case	Buses	Branches	Generators
1	9	9	3
2	39	46	10
3	118	186	54
4	300	411	69
5	500	597	90
6	2000	3206	544
7	3120	3693	505
8	10000	12706	2485
9	25000	32230	4834

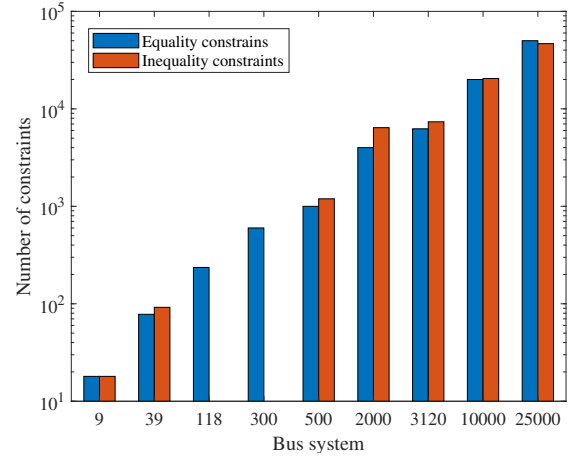
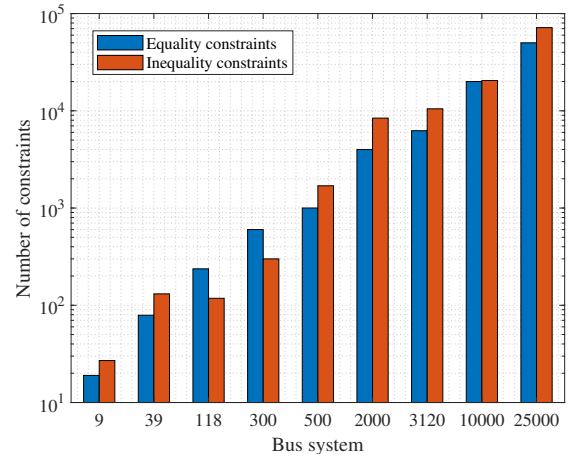
lems. It utilizes primal-dual interior point and line search filter based methods to find the solution. All the performance tests were done in a Macintosh environment with 2.6 GHz Intel Core i7 processor, 8 GB 1600 MHz DDR3 RAM, NVIDIA GeForce GT 650M 1024 MB and Intel HD Graphics 4000 1536 MB graphics card.

The formulation of a problem plays a key role in determining the solution methodology and processing time. This section compares the system model characteristics of the three formulation of AC-OPF. The number of variables in the ACOPF formulation of the different bus systems are shown in figure 1. An idea about the complexity associated with the ACOPF problem can be seen from this figure. A 9 bus system only has 24 variables while a 25,000 bus system have 59,668 variables in the optimization model. For a test system, the number of variables remain the same for all the three AC-OPF formulations.

**Figure 1:** Number of variables in the formulation

The equality and inequality constraints in the Polar and Cartesian formulation are depicted in the figures 2 and 3. The graphs are plotted in logarithmic scale to show the variations from smaller bus systems. The line flow limits in the case of 118 and 300 bus systems are very high and limits will not be exceeded irrespective of the optimized value. Therefore the line flow constraints can be excluded in polar for-

mulations as shown in figure 2.

**Figure 2:** Number of constraints in the power balance Polar formulation.**Figure 3:** Number of constraints in the power balance Cartesian formulation

The number of iterations for the code run to get the solution are shown in fig. 4. The Power balance Cartesian formulation is outperforming the other two formulations in smaller bus systems (9 bus, 118 bus, 500 bus) but in bigger bus systems (10K bus, 25K bus) its taking almost the same iterations as the current balance Cartesian formulation. The fig. 6 depicts the iteration numbers for the three formulations with current balance Cartesian values normalized to 1. The optimization code run-time is shown in fig. 5, power balance polar form is performing better in smaller bus system while current balance Cartesian formulation is running with least time for the biggest bus system considered for this study (25K). The improved performance for the current balance Cartesian form for bigger bus system can be clearly seen in figure fig. 6. The performance seems to be increasing with increasing number of buses in the network or with increasing complexity. To understand the modeling framework in a bit more detail, the Jacobian and hessian values in the for-

mulation are also noted. The values are shown in table 5 and the figure with current balance values normalized to 1 is plotted in fig. 8. The acronym Equality (P) stands for the equality constraint Jacobian in power balance Polar formulation, Equality (C) denote equality constraint Jacobian in power balance Cartesian form and similarly for the Inequality terms. The power balance Cartesian and current balance Cartesian show equal or very similar values but power balance polar has lesser values in most cases. The table 5 in appendix list all the values for the the formulations.

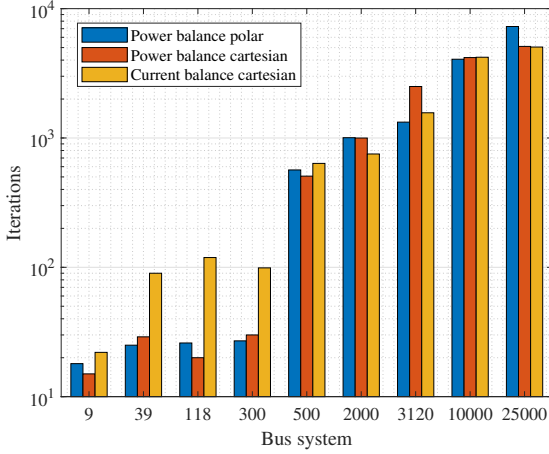


Figure 4: Iterations required to complete the code run

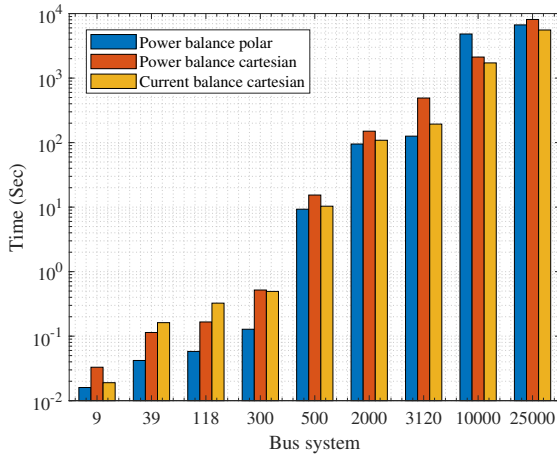


Figure 5: Run time comparison

The results from the code are compared with MATPOWER simulation to check the validity of the results. MATPOWER is an open-source power flow simulations package that provides power flow, OPF, AC-OPF and other tools targeted towards researchers and students [49, 30]. MATPOWER is run in a GNU Octave environment for the power flow simulation with all the cases tested and compared with final objective value [18]. MATPOWER utilized the MIPS [47] and in polar balance polar formulation for the analysis. The results are shown in table 3, the final objective value from both

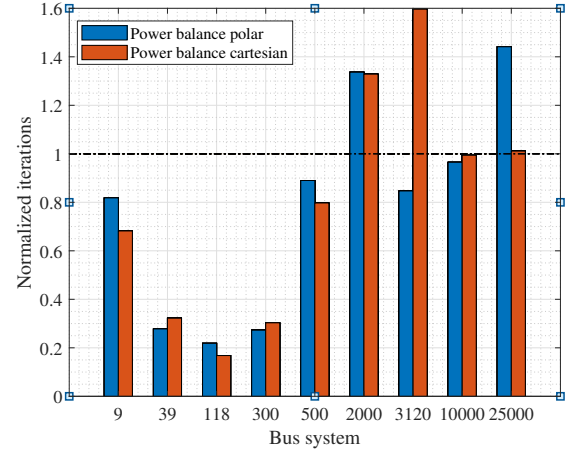


Figure 6: No. of Iterations with current balance iterations normalized to 1

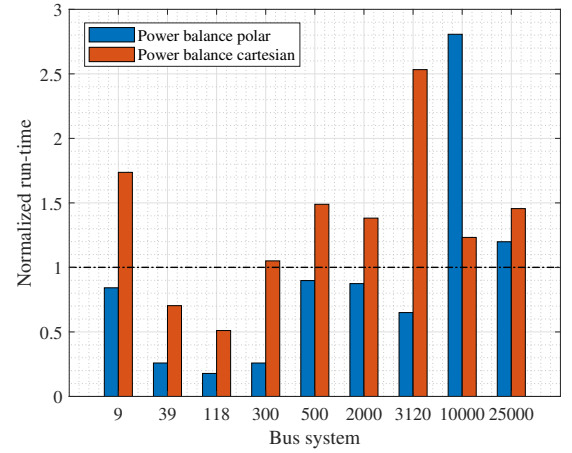


Figure 7: Run-time with current balance run-time normalized to 1

the code run and the MATPOWER simulation matches exactly, except for a few small variation in the decimal value.

Table 3

Objective value comparison with MATPOWER output.

Bus System	MATPOWER	Code
9	5296.69	5297.406
39	41864.18	41864.177
118	129660.7	129660.684
300	719725.11	719725.098
500	72578.3	72578.295
2000	$1.2288 * 10^6$	$1.2288 * 10^6$
3120	$2.1427 * 10^6$	$2.1427 * 10^6$
10000	$2.4858 * 10^6$	$2.4858 * 10^6$
25000	$6.0178 * 10^6$	$6.0178 * 10^6$

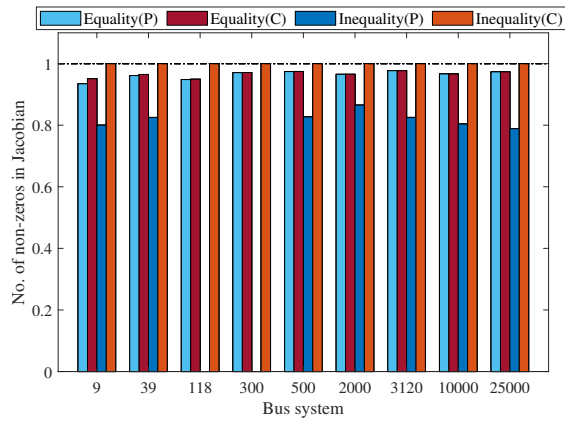


Figure 8: Number of non-zeros in Jacobian with Current balance Cartesian values normalized to 1.

6. Observations and Conclusion

This paper presented a computational and performance evaluation of three different AC-OPF formulations: power balance polar, power balance Cartesian and current balance Cartesian. The formulations were tested with a wide variety of bus systems ranging from smaller bus systems (9 bus) to larger bus (25,000 bus) system models. A steady increase in problem complexity (eg: number of variables and constraints in the model) with increasing bus number can be identified from this study. The three formulations converged to the same final solution even though with varying number of iterations and run-time.

Power balance polar form showed the best computational time for smaller bus systems while the current balance Cartesian form showed promising improvement in computational time with increasing problem complexity, outperforming the other two formulation for the 25,000 bus system case. The results show a similar pattern for the iterations with power balance polar having the least iteration number for smaller bus system while current balance Cartesian performed the least iteration number for the 25k bus system.

The validity of the results is tested in matpower for all the cases. The values of non-zeros in equality constraint Jacobian, inequality constraint Jacobian and lagrangian Hessian in the problem formulation are noted to evaluate the three formulations. The current balance Cartesian formulation had the largest number of non-zeros in the equality and inequality constraint Jacobian matrix closely followed by the power balance Cartesian formulation. In the case of non-zeros in Hessian matrix, all the three formulations had the same number of non-zero values.

A. My Appendix

References

[1] Akbari, T., Bina, M.T., 2016. Linear approximated formulation of AC optimal power flow using binary discretisation. *IET Generation, Transmission and Distribution* 10, 1117–1123. doi:10.1049/iet-gtd.2015.0388.

[2] Araujo, L.R., Penido, D.R., Carneiro, S., Pereira, J.L., 2013. A three-

phase optimal power-flow algorithm to mitigate voltage unbalance. *IEEE Transactions on Power Delivery* 28, 2394–2402. doi:10.1109/TPWRD.2013.2261095.

[3] Athay, T., Podmore, R., Virmani, S., 1979. A practical method for the direct analysis of transient stability. *IEEE Transactions on Power Apparatus and Systems PAS-98*, 573–584. doi:10.1109/TPAS.1979.319407.

[4] Balay, S., Abhyankar, S., Adams, M.F., Brown, J., Brune, P., Buschelman, K., Dalcin, L., Dener, A., Eijkhout, V., Gropp, W.D., Karpeyev, D., Kaushik, D., Knepley, M.G., May, D.A., McInnes, L.C., Mills, R.T., Munson, T., Rupp, K., Sanan, P., Smith, B.F., Zampini, S., Zhang, H., Zhang, H., 2020. PETSc Users Manual. Technical Report ANL-95/11 - Revision 3.13. Argonne National Laboratory. URL: <https://www.mcs.anl.gov/petsc>.

[5] Balay, S., Abhyankar, S., Adams, M.F., Brown, J., Brune, P., Buschelman, K., Dalcin, L., Dener, A., Eijkhout, V., Gropp, W.D., Karpeyev, D., Kaushik, D., Knepley, M.G., May, D.A., McInnes, L.C., Mills, R.T., Munson, T., Rupp, K., Sanan, P., Smith, B.F., Zampini, S., Zhang, H., Zhang, H., 2019. PETSc Web page. <https://www.mcs.anl.gov/petsc>. URL: <https://www.mcs.anl.gov/petsc>.

[6] Baradar, M., Hesamzadeh, M.R., 2015. AC power flow representation in conic format. *IEEE Transactions on Power Systems* 30, 546–547. doi:10.1109/TPWRS.2014.2326980.

[7] Birchfield, A.B., Xu, T., Gegner, K.M., Shetye, K.S., Overbye, T.J., 2017. Grid Structural Characteristics as Validation Criteria for Synthetic Networks. *IEEE Transactions on Power Systems* 32, 3258–3265. doi:10.1109/TPWRS.2016.2616385.

[8] Cain, M.B., O'Neill, R.P., Castillo, A., 2012. History of Optimal Power Flow and Formulations. Technical Report.

[9] Carpentier, J., 1979. Optimal power flows. *International Journal of Electrical Power and Energy Systems* 1, 3–15. doi:10.1016/0142-0615(79)90026-7.

[10] Castillo, A., 2016. Essays on the ACOPF problem: formulations, approximations, and applications in the electricity markets. Ph.D. thesis.

[11] Castillo, A., Lipka, P., Watson, J.P., Oren, S.S., O'Neill, R.P., 2016. A Successive Linear Programming Approach to Solving the IV-ACOPF. *IEEE Transactions on Power Systems* 31, 2752–2763. doi:10.1109/TPWRS.2015.2487042.

[12] Chatzivasileiadis, S., 2018. Optimization in Modern Power Systems. Technical Report September. Technical University of Denmark (DTU). URL: <http://arxiv.org/abs/1811.00943>, arXiv:1811.00943.

[13] Chow, J.H., 1982. Time-Scale Modeling of Dynamic Networks with Applications to Power Systems. Springer-Verlag.

[14] Coffrin, C., Hijazi, H.L., Van Hentenryck, P., 2016. The QC Relaxation: A Theoretical and Computational Study on Optimal Power Flow. *IEEE Transactions on Power Systems* 31, 3008–3018. doi:10.1109/TPWRS.2015.2463111, arXiv:1502.07847.

[15] Cvijic, S., Feldmann, P., Hie, M., 2012. Applications of homotopy for solving AC power flow and AC optimal power flow, in: *IEEE Power and Energy Society General Meeting*. doi:10.1109/PESGM.2012.6345453.

[16] Da Costa, V.M., Rosa, A.L., 2008. A comparative analysis of different power flow methodologies, in: *2008 IEEE/PES Transmission and Distribution Conference and Exposition: Latin America*, IEEE. pp. 1–7. doi:10.1109/TDC-LA.2008.4641868.

[17] Dkhil, N., Eynard, J., Thil, S., Grieco, S., 2020. A survey of modelling and smart management tools for power grids with prolific distributed generation. *Sustainable Energy, Grids and Networks* 21, 100284. URL: <https://doi.org/10.1016/j.segan.2019.100284>, doi:10.1016/j.segan.2019.100284.

[18] Eaton, J., Batema, D., Hauberg, S., Wehbring, R., 2019. GNU Octave version 5.1.0 manual: a high-level interactive language for numerical computations. Technical Report. URL: <https://www.gnu.org/software/octave/doc/v5.1.0/>.

[19] Farivar, M., Low, S.H., 2013. Branch flow model: Relaxations and convexification-part i. *IEEE Transactions on Power Systems* 28, 2554–2564. doi:10.1109/TPWRS.2013.2255317, arXiv:1204.4865.

Table 4
AC-OPF Results.

Test case	Parameters	Power Balance Polar	Power Balance Cartesian	Current Balance Cartesian
9- Bus system	Objective value	5297.406	5297.406	5297.406
	Iterations	18	15	22
	Time (secs)	0.016	0.033	0.019
39-Bus system	Objective value	41864.177	41864.177	41864.177
	Iterations	25	29	90
	Time (secs)	0.042	0.114	0.162
118-Bus system	Objective value	129660.68	129660.68	129660.68
	Iterations	26	20	119
	Time (Secs)	0.058	0.166	0.325
300-Bus system	Objective value	719725.1	719725.1	719725.1
	Iterations	27	30	99
	Time (Secs)	0.128	0.519	0.494
500 Bus system	Objective value	72578.295	72578.295	72578.295
	Iterations	566	507	636
	Time (Secs)	9.284	15.396	10.338
2000 Bus system	Objective value	$1.23 * 10^6$	$1.23 * 10^6$	$1.23 * 10^6$
	Iterations	1005	999	752
	Time (Secs)	95.121	150.327	108.77
3120 Bus System	Objective value	$2.1427 * 10^6$	$2.1427 * 10^6$	$2.1427 * 10^6$
	Iterations	1326	2500	1566
	Time (secs)	125.93	490.638	193.714
10,000 Bus System	Objective value	$2.4858 * 10^6$	$2.4858 * 10^6$	$2.4858 * 10^6$
	Iterations	4063	4185	4210
	Time (secs)	4824.988	2118.738	1719.023
25,000 Bus System	Objective value	$6.017 * 10^6$	$6.017 * 10^6$	$6.017 * 10^6$
	Iterations	7276	5105	5048
	Time (secs)	6672.571	8102.079	5565.438

- [20] Fioretto, F., Mak, T.W.K., Van Hentenryck, P., 2019. Predicting AC Optimal Power Flows: Combining Deep Learning and Lagrangian Dual Methods. arXiv:1909.10461 URL: <http://arxiv.org/abs/1909.10461>, arXiv:1909.10461.
- [21] Frank, S., Rebennack, S., 2012. A Primer on Optimal Power Flow : Theory , Formulation , and Practical Examples. Technical Report October. URL: <http://econbus.mines.edu/working-papers/wp201214.pdf>.
- [22] Jereminov, M., Pandey, A., Pileggi, L., 2019. Equivalent circuit formulation for solving ac optimal power flow. IEEE Transactions on Power Systems 34, 2354–2365. doi:10.1109/TPWRS.2018.2888907.
- [23] Kardos, J., Kourounis, D., Schenk, O., Zimmerman, R., 2018. Complete results for a numerical evaluation of interior point solvers for large-scale optimal power flow problems. Technical Report. URL: <http://arxiv.org/abs/1807.03964>, arXiv:1807.03964.
- [24] Lin, W.M., Huang, C.H., Zhan, T.S., 2008. A hybrid current-power optimal power flow technique. IEEE Transactions on Power Systems 23, 177–185. doi:10.1109/TPWRS.2007.913301.
- [25] Liu, Y., Qu, Z., Xin, H., Gan, D., 2017. Distributed Real-Time Optimal Power Flow Control in Smart Grid. IEEE Transactions on Power Systems 32, 3403–3414. doi:10.1109/TPWRS.2016.2635683.
- [26] Madani, R., Sojoudi, S., Lavaei, J., 2015. Convex relaxation for optimal power flow problem: Mesh networks. IEEE Transactions on Power Systems 30, 199–211. doi:10.1109/TPWRS.2014.2322051.
- [27] Mhanna, S., Verbic, G., Chapman, A.C., 2019. Adaptive ADMM for distributed ac optimal power flow. IEEE Transactions on Power Systems 34, 2025–2035. doi:10.1109/TPWRS.2018.2886344.
- [28] Moreno, R., Obando, J., Gonzalez, G., 2019. An integrated OPF dispatching model with wind power and demand response for day-ahead markets. International Journal of Electrical and Computer Engineering 9, 2794–2802. doi:10.11591/ijece.v9i4.pp2794-2802.
- [29] Mühlpfordt, T., Faulwasser, T., Hagenmeyer, V., 2018. A generalized framework for chance-constrained optimal power flow. Sustainable Energy, Grids and Networks 16, 231–242. URL: <https://doi.org/10.1016/j.segan.2018.08.002>, doi:10.1016/j.segan.2018.08.002, arXiv:1803.08299.
- [30] Murillo-Sánchez, C.E., Zimmerman, R.D., Lindsay Anderson, C., Thomas, R.J., 2013. Secure planning and operations of systems with stochastic sources, energy storage, and active demand. IEEE Transactions on Smart Grid 4, 2220–2229. doi:10.1109/TSG.2013.2281001.
- [31] Nair, A.S., Hossen, T., Campion, M., Ranganathan, P., 2018a. Optimal Operation of Residential EVs using DNN and Clustering based Energy Forecast, in: 2018 North American Power Symposium, NAPS 2018, IEEE, pp. 1–6. doi:10.1109/NAPS.2018.8600628.
- [32] Nair, A.S., Hossen, T., Campion, M., Selvaraj, D.F., Goveas, N., Kaabouch, N., Ranganathan, P., 2018b. Multi-Agent Systems for Resource Allocation and Scheduling in a Smart Grid. Technology and Economics of Smart Grids and Sustainable Energy 3. doi:10.1007/s40866-018-0052-y.
- [33] Ochoa, L.F., Harrison, G.P., 2010. Using AC optimal power flow for DG planning and optimisation, in: IEEE PES General Meeting, PES 2010, IEEE, pp. 1–7. doi:10.1109/PES.2010.5589482.
- [34] O'Neill, R.P., Castillo, A., Cain, M.B., 2012. The IV formulation and linear approximations of the AC optimal power flow problem (OPF Paper 2). FERC Staff Technical Paper , 1–18URL: <http://www.ferc.gov/industries/electric/indus-act/market-planning/opf-papers/acopf-2-iv-linearization.pdf>.
- [35] Park, B., Tang, L., Ferris, M.C., Demarco, C.L., 2017. Examination of Three Different ACOPF Formulations with Generator Capability Curves. IEEE Transactions on Power Systems 32, 2913–2923. doi:10.1109/TPWRS.2016.2626142.
- [36] Sereeter, B., Vuik, C., Witteveen, C., Palensky, P., 2019. Optimal power flow formulations and their impacts on the performance of solution methods, in: IEEE Power and Energy Society General Meeting.

Table 5
Number of non-zeros in Jacobian and Hessian.

Test case	No. of non-zeros	Power balance polar	Power balance Cartesian	Current balance Cartesian
9 Bus System	Equality constraint Jacobian	114	116	122
	Inequality constraint Jacobian	72	90	90
	Lagrangian Hessian	96	96	96
39 Bus System	Equality constraint Jacobian	544	546	566
	Inequality constraint Jacobian	368	446	446
	Lagrangian Hessian	415	415	415
118 Bus System	Equality constraint Jacobian	2012	2014	2122
	Inequality constraint Jacobian	0	236	236
	Lagrangian Hessian	2408	2408	2408
300 Bus System	Equality constraint Jacobian	4610	4612	4750
	Inequality constraint Jacobian	0	600	600
	Lagrangian Hessian	3591	3591	3591
500 Bus System	Equality constraint Jacobian	6852	6854	7034
	Inequality constraint Jacobian	4776	5776	5776
	Lagrangian Hessian	4826	4826	4826
2000 Bus System	Equality constraint Jacobian	30424	30426	31524
	Inequality constraint Jacobian	25648	29648	29648
	Lagrangian Hessian	24552	24552	24552
3120 Bus System	Equality constraint Jacobian	42962	42964	43974
	Inequality constraint Jacobian	29448	35688	35688
	Lagrangian Hessian	35923	35923	35923
10000 Bus System	Equality constraint Jacobian	142706	142708	147678
	Inequality constraint Jacobian	81952	101952	101952
	Lagrangian Hessian	119755	119755	119755
25000 Bus System	Equality constraint Jacobian	350548	350550	360218
	Inequality constraint Jacobian	186640	236640	236640
	Lagrangian Hessian	269342	269342	269342

doi:10.1109/PESGM40551.2019.8973585.

- [37] Shchetinin, D., De Rubira, T.T., Hug, G., 2017. Conservative linear line flow constraints for AC optimal power flow, in: 2017 IEEE Manchester PowerTech, Powertech 2017, IEEE. pp. 1–6. doi:10.1109/PTC.2017.7981156.
- [38] Shchetinin, D., De Rubira, T.T., Hug, G., 2019. On the Construction of Linear Approximations of Line Flow Constraints for AC Optimal Power Flow. IEEE Transactions on Power Systems 34, 1182–1192. doi:10.1109/TPWRS.2018.2874173.
- [39] Shults, R.R., Sun, D.T., 1982. Optimal power flow based on P–Q decomposition. IEEE Trans Power Appar Syst PAS-101, 745–51.
- [40] Soares, T., Bessa, R.J., Pinson, P., Morais, H., 2018. Active distribution grid management based on robust AC optimal power flow. IEEE Transactions on Smart Grid 9, 6229–6241. doi:10.1109/TSG.2017.2707065.
- [41] Tang, Y., Dvijotham, K., Low, S., 2017. Real-Time Optimal Power Flow. IEEE Transactions on Smart Grid 8, 2963–2973. doi:10.1109/TSG.2017.2704922.
- [42] Tinney, W.F., 1968. Optimal Power Flow Solutions. IEEE Transactions on Power Apparatus and Systems PAS-87, 1866–1876.
- [43] Venzke, A., Chatzivasileiadis, S., Molzahn, D.K., 2019. Inexact Convex Relaxations for AC Optimal Power Flow: Towards AC Feasibility. arXiv:1902.04815, 1–11 URL: <http://arxiv.org/abs/1902.04815>, arXiv:1902.04815.
- [44] Venzke, A., Halilbasic, L., Markovic, U., Hug, G., Chatzivasileiadis, S., 2018. Convex Relaxations of Chance Constrained AC Optimal Power Flow. IEEE Transactions on Power Systems 33, 2829–2841. doi:10.1109/TPWRS.2017.2760699, arXiv:1702.08372.
- [45] Vovos, P.N., Bialek, J.W., 2006. Optimal power flow as a generation expansion and network reinforcement planning tool, in: 2006 IEEE Power Engineering Society General Meeting, PES. doi:10.1109/pes.2006.1709498.
- [46] Wachter, A., On, L.T.B., 2006. On the implementation of an interior-point filter line-search algorithm for large-scale nonlinear programming. Mathematical Programming 106, 25–57. doi:10.1007/s10107-004-0559-y.
- [47] Wang, H., Murillo-Sánchez, C.E., Zimmerman, R.D., Thomas, R.J., 2007. On computational issues of market-based optimal power flow. IEEE Transactions on Power Systems 22, 1185–1193. doi:10.1109/TPWRS.2007.901301.
- [48] Worighi, I., Maach, A., Hafid, A., Hegazy, O., Van Mierlo, J., 2019. Integrating renewable energy in smart grid system: Architecture, virtualization and analysis. Sustainable Energy, Grids and Networks 18. doi:10.1016/j.segan.2019.100226.
- [49] Zimmerman, R.D., Murillo-Sánchez, C.E., Thomas, R.J., 2011. MATPOWER: Steady-state operations, planning, and analysis tools for power systems research and education. IEEE Transactions on Power Systems 26, 12–19. doi:10.1109/TPWRS.2010.2051168.